IEEE Photonics Journal
An IEEE Photonics Society Publication

Open Access

A Modeling Investigation on High-Speed Broad Spectrum Filtering System Based on Electric Fluid Technology

Volume 9, Number 3, June 2017

Jun Wu
Qiuyue Zhu
Zhiyang Qi
Jun Xia
Chenliang Chang
Qilong Wang
Baoping Wang

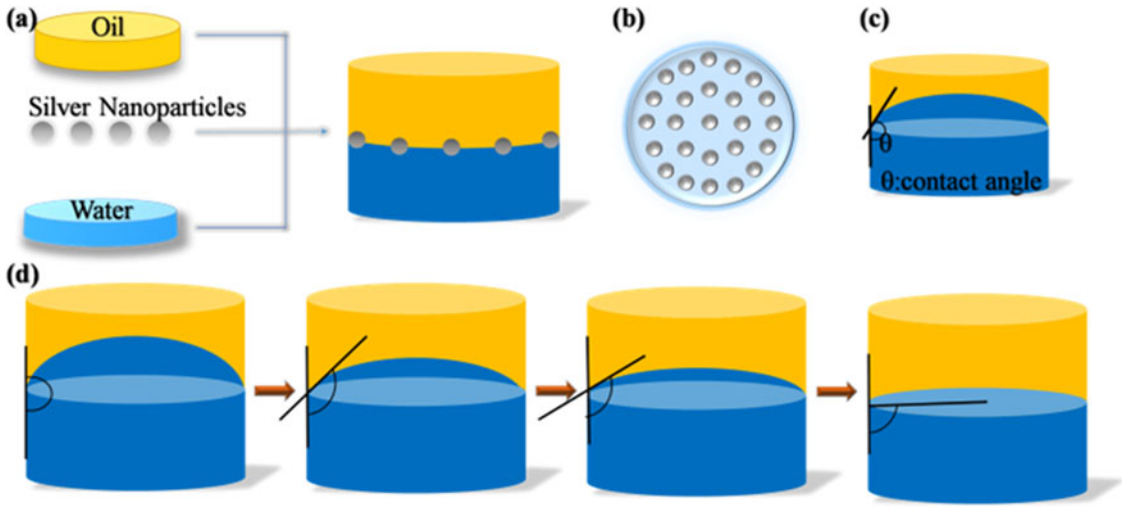

DOI: 10.1109/JPHOT.2017.2657749
1943-0655 © 2017 IEEE

A Modeling Investigation on High-Speed Broad Spectrum Filtering System Based on Electric Fluid Technology

Jun Wu, Qiuyue Zhu, Zhiyang Qi, Jun Xia, Chenliang Chang, Qilong Wang, and Baoping Wang

Joint International Research Laboratory of Information Display and Visualization, School of Electronic Science and Engineering, Southeast University, Nanjing 210096, China

DOI:10.1109/JPHOT.2017.2657749

Manuscript received December 22, 2016; revised January 14, 2017; accepted January 18, 2017. Date of publication March 2, 2017; date of current version April 25, 2017. This work was supported in part by the National Natural Science Foundation of China (NSFC) under Grant 61306140, Grant 61372030, Grant 61571124, and Grant 91333118; in part by the Natural Science Foundation of Jiangsu Province (BK20130618); in part by the NSFC major international (regional) research project (51120125001); in part by the NSFC Research Fund for International Young Scientists (61550110243); in part by the National Basic Research Program of China under Grant 2013CB328803; in part by the National High Technology Research and Development Program of China under Grant 2015AA016301; and in part by the Fundamental Research Funds for the Central Universities under Grant 2242015KD004. Corresponding author: J. Wu (e-mail: wujunseu@seu.edu.cn).

Abstract: By combining advanced fluid control technology with surface plasmonic resonance phenomenon, we could take advantage of various unique characteristics of plasmonics without changing the original structure to realize a tunable color filtering system. By modifying the wetting properties of solid surface with an electric field, electro-fluid control technology could tune the curvature of two-phase fluid interface continuously and, therefore, change the distributions of silver nanoparticles on the interface accordingly. Based on this fluidic optical design, we investigated the influencing factors of color filtering performance by modeling, finally got an optimized design to achieve broad spectrum filtering system. As the color filtering function is realized simply and rapidly by charging, and therefore, this design could improve the efficiency of the electro-optical systems and is a promising idea for many applications, such as the dynamic display devices.

Index Terms: Modeling, tunable filters, electrowetting, plasmonics, electro-optical systems.

1. Introduction

Surface plasmonic polaritons (SPPs), which could achieve strong enhancement in localized electric fields and break through the subwavelength diffraction limit of conventional optics, have attracted researchers' great attention in many fields [1]–[3]. Many plasmonic structures have been reported for their ability to sustain resonance bands for filtering applications [4]–[10], such as nano grating arrays [11], nano hole arrays [12]–[14] and other nanostructures [15]–[18]. These structures can filter a specific color by tuning the resonant absorption or transmission peak at the visible range. However, most of these designs are structure-based, which means the colors filtered are highly dependent on the structure parameters such as diameters, height, thickness width, and so on. Besides, the colors filtered are usually limited in a small range of the visible spectrum. Although Zhang *et al.* experimented and reported a design to use nematic liquid crystals to control the metal

nanoparticle's dispersion, alignment, and assembly and make applications in switchable plasmonic color filters and E-Polarizers [19], However, based on the action principle of liquid crystals, reversing liquid crystal molecules takes time. Besides, the response of liquid crystals is limited by temperature. When the temperature is low, the liquid crystals' respond time increases rapidly and is not suitable for the applications with high demands in tuning speed, such as video players, and so on.

This article aims to design a kind of color filtering system with two-phase fluid and silver nanoparticles, the absorption peak of which could be adjusted in the whole visible spectrum range continuously and rapidly. In order to realize this function, we introduced an advanced fluid control technology named electrowetting [20]–[23], which is now widely used as driving method for fluid and Electro Optic devices, and based on the work of Moghaddam *et al.*, we found the electrowetting technology could adjust the curvature of water/oil interface efficiently by modifying the wetting properties of solid surface with an electric field [24]. Meanwhile, the distribution of the silver nanoparticles on the two-phase fluid interface changed accordingly. In order to assure the silver nanoparticles could be evenly distributed at water-oil interface, we should also use emulsion to prevent these particles from sedimentation and agglomeration [25], [26]. A modeling investigation is performed to prove the validity of this novel design. Furthermore, by selecting suitable particle size and initial distribution density, an optimized design to achieve broad spectrum filtering system is proposed. We believe that by combining the electrowetting technology and SPPs, we could find new applications in the field of novel electro-optical systems, such as fluidic display devices.

2. Modeling

The technology used in this article to adjust the absorption peak of silver nanoparticles is named Electrowetting. With two electrodes charged on different sides, this technology can be used to modify the interfacial energy between polarized fluid and conductive solid surface, and therefore get the water and oil interface changed in our model. Please note that, the silver nanoparticle behaves differently in different solutions and in different interfaces [27], in this stimulation work, we only focus on the water-oil interface. The equation below is the relationship between voltage and contact angel:

$$\cos\theta - \cos\theta_0 = \frac{\varepsilon_0 \varepsilon_r}{2 d_H \gamma} U^2.$$

θ is the contact angel under certain voltage, and θ_0 is the original contact angel. ε_0 is the permittivity of vacuum, ε_r is the permittivity of the fluid, d_H is the thickness of dielectric film, γ is the interface energy, and U is the charged voltage.

Here, we presented our experimental model in Fig. 1. From Fig. 1(a), we could get the main structure of the model used in this article. Silver particles were placed uniformly on the water/oil interface, as can be observed in Fig. 1(b). By adjusting the voltage between two electrodes, the contact angles as indicated in Fig. 1(c) can be changed. Supposing that the original water/oil interface is a hemisphere surface, the initial contact angel is 180 degree. Actually, the real initial contact angel of water-oil interface should be less than 180 degree. While, here, we use ideal model for stimulation work, and we assume that the initial contact angel is extremely close to 180 degree, so we use 180 degree to simplify our calculation steps. As is indicated in Fig. 1(d), by adding the voltage between two electrodes, we could modify the interface from hemisphere surface *to* ellipsoidal surface, and finally get a circle plane after the contact angel being reduced to 90 degree.

Let's assume that the radius of the cylinder model is r nm, and the number of particles is n. When the contact angel is 180 degrees, the period of each two particle is given by

$$\mathrm{d} = \sqrt{\frac{2\pi r^2}{n}}$$

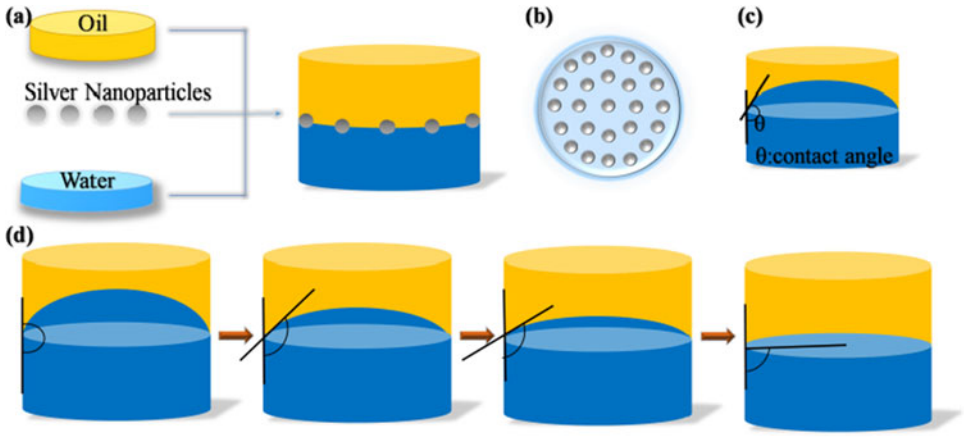

Fig. 1. (a) Main structure of the model. (b) Vertical view of the model which indicates the distribution of nanoparticles. (c) Defination of contact angle. (d) Changing trends of contact angles after charging.

when the contact angel is reduced to 90 degrees, the period of each two particles is expressed as

$$d' = \sqrt{\frac{\pi r^2}{n}}$$

then we could find that

$$d = \sqrt{2}d'.$$

The equation we get here indicates that we could simply utilize electrowetting technology to adjust the original period of the silver particles from d nm to d/1.4 nm. As we all know that, the absorption peak of silver particles is deeply affected by the particle period, so it is hopefully to get the peak adjusted continuously in our design. In order to take full advantage of such effect, we should find out a certain kind of silver particles with proper diameter, period range and initial distribution, to realize the switchable absorption band in a broad visible spectrum range. Specifically, the finite difference time domain method (FTDT) is used in our modeling investigation.

3. Results and Data Analyzing

After designing the model we have mentioned above, we started a large amount of stimulation work to find a proper diameter and period range for the silver particles. We firstly determined the refractive index of water, oil, and the silver metal particles. In this work, the refractive index of oil is around 1.7, water is 1.33, and silver's refractive index is modelled in Drude model around visible spectrum, which is taken into account in our stimulation circumstance. Besides, actual refractive index changes with wavelength, however the effect is tiny and we aimed to design a ideal model for stimulation, so we ignore this distinction in our stimulation work. By setting a constant particle diameter, and modifying the particle period, the initial wavelengths and intensity of the plasmonic resonances can be determined. Then by limiting the range of period from d to d/1.4, the range of the absorption peak moved can be calculated. After that we change the diameter and repeat the work mentioned above. Finally, we compared the data we got and found out a desired property for our design.

Fig. 2 indicates below shows our stimulation results of 50 nm, 80 nm, 120 nm, 160 nm, 200 nm, 250 nm silver nanoparticles, and the area between two black dash lines is the range the absorption peak moved from period d to d/1.4 (from right to left).

In Fig. 2(a), we used silver particles with 50 nm diameter and set the original period d as 250 nm, and then we changed the period of particles until it decreases to 180 nm. From the figure we could

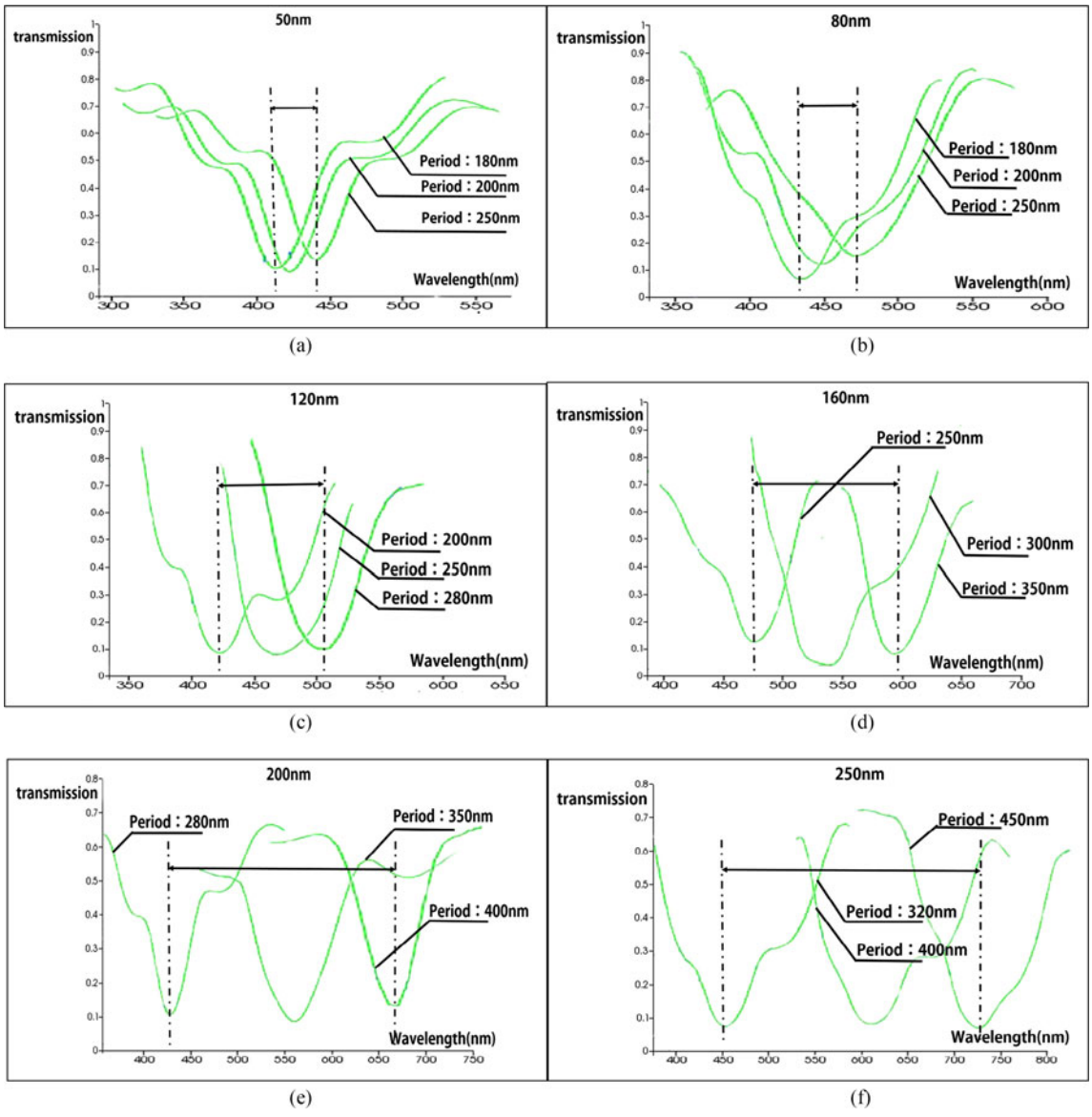

Fig. 2. Silver particles with different diameters and their absorption band in different periods. (a) Diameter: 50 nm. (b) Diameter: 80 nm. (c) Diameter: 120 nm. (d) Diameter: 160 nm. (e) Diameter: 200 nm. (f) Diameter: 250 nm

see the absorption peak of 50 nm particles only moved 35 nm in wavelength, from 410 nm to about 445 nm. From this stimulation result, we could prove the validity of this novel design, although the range the absorption peak moved is quite small. When the diameter of nanoparticles decline, the electrons escape from the surface of nanoparticles and conduct to the affinity energy level of the substrate, which means that the density of electrons decrease, and the frequency of free electron plasma (wp) decrease as well. Because the frequency of SPR (wsp) is proportional to wp, so the absorption peak moves to the left of the original one. Therefore, we decide to increase the diameter of these particles so that we could get a wider range of absorption wavelength. In Fig. 2(b), we changed the diameter of silver particles to 80 nm and repeated our stimulation from period 180 nm to 250 nm. The absorption peak changed a little compared to that of 50 nm particles, which moved from 435 nm to 470 nm. From this result, we could find although the peak moved

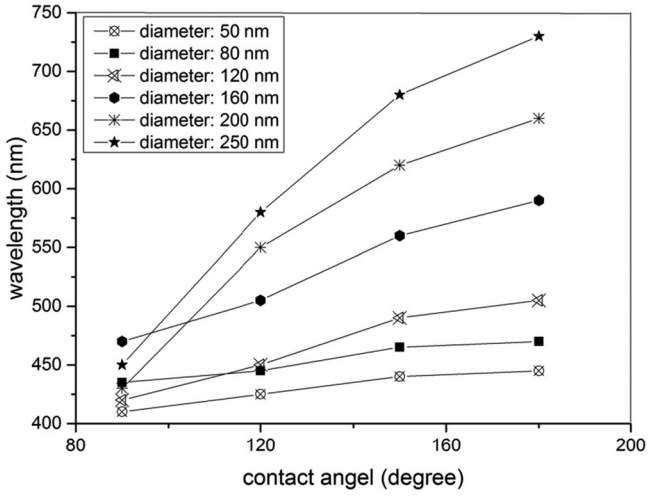

Fig. 3. Relationship between contact angel and the absorption peak wavelength.

to a larger wavelength area, the range did not change, maintaining 35 nm. In Fig. 2(c), we then used particles with 120 nm diameter and changed the range of period as well, because the SPR should be considered in a proper range of period between each two particles. If the period is too small relative to the diameter, the absorption peak may move out of the range of visible light, and when the period is too large, the interaction of two particles could be very small. In Fig. 2(c), the absorption peak of 200 nm period is 420 nm, and that of 280 nm period is 505 nm. The peak moved 85 nm, which is much larger than that in both Fig. 2(a) and (b). In Fig. 2(d)–(f), we kept changing the diameter of particles to 160 nm, 200 nm, and finally 250 nm, and the period of them became larger accordingly. The absorption peak moved to a larger wavelength and the area between two black dash lines also becomes wider. When diameter is 160 nm, the absorption peak moved from 470 nm to 590 nm. When the diameter is 200 nm, the absorption peak is from 430 nm to 660 nm. In Fig. 2(f), we used silver particles with 250 nm diameter. When the period is 320 nm, the absorption peak is 450 nm, and when it changed to 450 nm, the absorption peak moved to 730 nm. The wavelength moved for 280 nm, which covers most range of visible light. As a result, we find a kind of silver particle which has suitable properties to realize broad spectrum filtering.

Fig. 3 below shows the relationship between contact angel and the absorption peak wavelength. By adjusting contact angel, while the diameter of particles is becoming larger, the absorption peak will change accordingly in a larger range.

We have proved above that the contact angel could control the particle period. From Fig. 3, we could have a clear view of how contact angel had effect on the movement of absorption peak. Moreover, the equation about electrowetting which we have mentioned above indicates that the contact angel changes with the applied voltage continuously. Finally, by charging voltage between electrodes, we can make the period change continuously.

After performing the stimulation work on particles with different properties, we collected a large number of calculated data, from which, several other findings about this design have been observed. Fig. 4 shows below is a line graph about the relationship between absorption peak wavelength and diameter in different periods.

Firstly, from the Fig. 4 we could find that different period has different distribution in the wavelength. Basically, the larger period could induce larger wavelength, and some small periods could let the wavelength of absorption peak centered in the low number. For instance, when period is 450 nm, the corresponding wavelengths of absorption peak are all bigger than 700 nm, and when it turns to 150 nm period, the biggest wavelength is only approximate 425 nm.

Second, we could also find all of these lines have a similar trend that the wavelength rises to a peak and then climbs down. The rising trend is mainly because that when we use a particle with

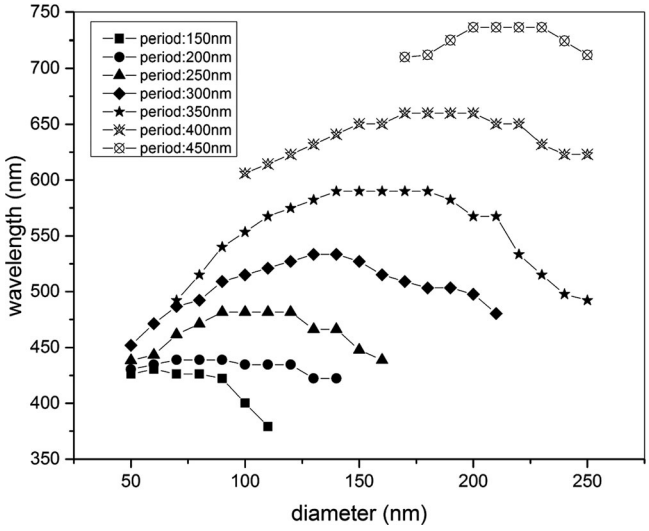

Fig. 4. Relationship between diameter and wavelength of absorption peak in different periods.

bigger diameter, the absorption band would move to a bigger wavelength, and the wavelength of the absorption peak will become bigger. As shown in Fig. 4, we can find that the fall-off happens roughly when period $=$ 2$*$diameter. We have mentioned above that when the diameter of nanoparticles increases, the absorption peak will have a red shift. When the diameter continuously becoming larger, the period between each two nanoparticles may become so small compared to the diameter that we cannot ignore the influence of coupling resonance between those two particles, which will lead to the blue-shift of absorption peak [28], [29].

Finally, we could also find when we fixed on a diameter and increase the period, the increment of wavelength is different. We could find that the increment by bigger diameter particle is larger than smaller one when we increase the period. From the Fig. 4 we can see that when diameter is 250 nm, the gap between every line is wide, but there is only tiny change when the diameter is 50 nm. This conclusion could also well prove why we should make the diameter larger during our experiment.

Besides, the data we got and these discussions and findings above are all based on our ideal model in stimulation work. Therefore, there may be some factors we have ignored in our stimulation work which would effect our system in real experiments. For example, the contact angel hysteresis has effects on the system, when the voltage changes, the contact angel's change may have some delay in time and also small distinction compared to the theoretical value. We will take this question into consideration in further real experiment and make some change in our model based on how the effects act.

4. Conclusion

By doing this stimulation and analyzing work, we finally find a certain kind of SPPs device design to make the absorption peak move nearly across the whole range of visible spectrum. More importantly, this new design is all dependent on voltage, and therefore, the response time could be very short and different colors can be filtered and substituted rapidly. Besides, we find some rules of how absorption peak changes with the diameters of the particles when they are distributed in different periods. All the findings we have here are based on the stimulation of our module and more real experiments are desired in the future to improve this design. By combining the electrowetting technology with SPR in plasmonics, we could find a new potential of controllable color display, which is promising for many applications in optics.

References

[1] A. V. Zayats, I. I. Smolyaninov, and A. A. Maradudin, "Nano-optics of surface plasmonpolaritons," *Phys. Rep.*, vol. 408, no. 3/4, pp. 131–314, 2005.
[2] D. Derkacs *et al.*, "Improved performance of amorphous silicon solar cells via scattering from surface plasmonpolaritons in nearby metallic nanoparticles," *Appl. Phys. Lett.*, vol. 89, no. 9, 2006, Art. no. 093103.
[3] W. L. Barnes, "Surface plasmonpolariton length scales: A route to sub-wavelength optics," *J. Opt. A Pure Appl. Opt.*, vol. 8, no. 8, pp. 87–93, 2006.
[4] B. Lee, H. Yun, and S. Lee, *Plasmonic Color Tuning*. San Francisco, CA, USA: SPIE, 2016.
[5] Z. Fang *et al.*, "Color-tuning and switching optical transport through CdS hybrid plasmonic waveguide," *Opt. Exp.*, vol. 17, no. 22, pp. 20327–20332, 2009.
[6] G. Si *et al.*, "Incident-angle dependent color tuning from a single plasmonic chip," *Nanotechno.*, vol. 25, no. 45, 2014, Art. no. 455203.
[7] S. D. Yun *et al.*, "Color filters, "plasmonic color filter and its fabrication for large-area applications," *Adv. Opt. Mater.*, vol. 1, no. 2, pp. 133–138, 2013.
[8] S. Albaladejo, J. J. Sáenz, and M. I. Marqués, "Plasmonic nanoparticle chain in a light field: A resonant optical sail," *Nano Lett.*, vol. 11, no. 11, pp. 4597–4560, 2011.
[9] T. Ellenbogen, S. Kwanyong, and B. C. Kenneth, "Chromatic plasmonic polarizers for active visible color filtering and polarimetry," *Nano Lett.*, vol. 12 no. 2, pp. 1026–1031, 2012
[10] H. F. Ma *et al.*, "Broadband and high-efficiency conversion from guided waves to spoof surface plasmonpolaritons," *Laser Photon. Rev.*, vol. 8, no. 1, pp. 146–151, 2014.
[11] P. Berini, "Long-range surface plasmonpolaritons," *Adv. Opt. Photon.*, vol. 1, no. 3, pp. 484–588, 2009.
[12] R. Ortuño *et al.*, "Role of surface plasmonpolaritons on optical transmission through double layer metallic hole arrays," *Pediatria Polska*, vol. 58, no. 2, pp. 149–152, 2015.
[13] M. Nakao *et al.*, "GaAs and InPnano-hole arrays fabricated by reactive beam etching using highly ordered alumina membranes," *Jpn. J. Appl. Phys.*, vol. 38, no. 28, pp. 781–784, 1999.
[14] R. Gordon *et al.*, "Strong polarization in the optical transmission through elliptical nanohole arrays," *Phys. Rev. Lett.*, vol. 92, no. 3, 2004, Art. no. 037401.
[15] A. R. Ferhan, J. A. Jackman, and N.-J. Cho, "Integration of quartz crystal microbalance-dissipation and reflection-mode localized surface plasmon resonance sensors for biomacromolecular interaction analysis," *Analyt. Chem*, vol. 24, no. 88, pp. 12524–12531, 2016.
[16] Y. Noh *et al.*, "Properties of the dye sensitized solar cell with localized surface plasmon resonance inducing Au Nano thin films," vol. 26, no. 8, pp. 417–421, 2016.
[17] A. Dhawan, M. Canva, and T. Vodinh, "Narrow groove plasmonicnano-gratings for surface plasmon resonance sensing," *Opt. Exp.*, vol. 19, no. 2, pp. 787–813, 2011.
[18] Y. Wang *et al.*, "Metamaterial-plasmonic absorber structure for high efficiency amorphous silicon solar cells," *Nano Lett.*, vol. 12, no. 1, pp. 440–445, 2012.
[19] Y. Zhang *et al.*, "Metal nanoparticle dispersion, alignment, and assembly in nematic liquid crystals for applications in switchable plasmonic color filters and e-polarizers," *ACS Nano*, vol. 9, no. 3, pp. 3097–3108, 2015.
[20] R. A. Hayes and B. J. Feenstra, "Video-speed electronic paper based on electrowetting," *Nature*, vol. 425, pp. 383–385, 2003.
[21] M. G. Pollack, R. B. Fair, and A. D. Shenderov, "Electrowetting-based actuation of liquid droplets for microfluidic applications," *Appl. Phys. Lett.*, vol. 77, no. 11, pp. 1725–1726, 2000.
[22] F. Mugele and J. C. Baret, "Electrowetting: From basics to applications," *J. Phys. Condens. Matter*, vol. 17, no. 28, pp. 705–774, 2005.
[23] S. K. Cho, H. Moon, and C. J. Kim, "Creating, transporting, cutting, and merging liquid droplets by electrowetting-based actuation for digital microfluidic circuits," *J. Microelectromech. Syst.*, vol. 12, no. 1, pp. 70–80, 2003.
[24] M. S. Moghaddam *et al.*, "Simulation, fabrication, and characterization of a tunable electrowetting-based lens with a wedge-shaped PDMS dielectric layer," *Appl. Opt.*, vol. 54, no. 10, pp. 3010–3017, 2015
[25] R. Kagawa *et al.*, "Oil-in-water emulsion as fabrication platform for uniform plasmon-controlled two-dimensional metallic nanoparticle array," *Appl. Phys. Exp.*, vol. 9 no. 7, 2016, Art. no. 075003.
[26] V. A. Turek *et al.*, "Plasmonic ruler at the liquid–liquid interface," *ACS Nano*, vol. 6, no. 9, pp. 7789–7799, 2012
[27] Z. Yang *et al.*, "LSPR properties of metal nanoparticles adsorbed at a liquid–liquid interface," *Phys. Chem. Chem. Phys.*, vol. 15, no. 15, pp. 5374–5378, 2013
[28] Z. Qi *et al.*, "Plasmon-enhanced energy transfer between quantum dots and tunable film-coupled nanoparticles," *J. Phys. D Appl. Phys.*, vol. 49, no. 23, 2016, Art. no. 235103.
[29] J. Zhang *et al.*, "Metal-enhanced single-molecule fluorescence on silver particle monomer and dimer: Coupling effect between metal particles," *Nano Lett.*, vol. 7, no. 7, pp. 2101–2107, 2007